

Supporting Information

for *Adv. Mater. Interfaces*, DOI: 10.1002/admi.202000931

Surface-Initiated Grafting of Dendritic Polyglycerol from Mussel-Inspired Adhesion-Layers for the Creation of Cell-Repelling Coatings

Michaël W. Kulka, Chuanxiong Nie, Philip Nickl, Yannic Kerkhoff, Arushi Garg, Dirk Salz, Jörg Radnik, Ingo Grunwald, and Rainer Haag**

Supporting Information for

Surface-Initiated Grafting of Dendritic Polyglycerol from Mussel-Inspired Adhesion Layers for the Creation of Biocompatible Cell-Repelling Coatings

Michaël W. Kulka,^a Chuanxiong Nie,^a Philip Nickl,^{a,b} Yannic Kerkhoff,^a Arushi Garg,^a Dirk Salz,^c Jörg Radnik,^b Ingo Grunwald,^{c,d} Rainer Haag*,^a

^a Institute for Chemistry and Biochemistry, Freie Universität Berlin, Takustraße 3, 14195 Berlin, Germany

^b BAM – Federal Institute for Material Research and Testing, Division of Surface Analysis and Interfacial Chemistry, Unter den Eichen 44-46, 12205 Berlin, Germany

^c Fraunhofer Institute for Manufacturing Technology and Advanced Materials IFAM, Wiener Straße 12, 28359 Bremen, Germany

^d Hochschule Bremen – City University of Applied Sciences, Department of Industrial and Environmental Biology, Neustadtswall 30, 28199 Bremen, Germany

1. EXPERIMENTAL SECTION

1.1. CHEMICALS & LAB TECHNIQUES

The chemicals were purchased from Merck (Darmstadt, Germany) and were used as received without further purification, unless mentioned otherwise. Besides, NaOH pellets bought from VWR International (Darmstadt, Germany). Non-protic solvents were either purchased in an extra-dry form or were dried with the help of CaH_2 , prior to use. Dialysis was performed using benzoylated cellulose tubes (D7884, width: 32 mm; molecular-weight cutoff (MWCO): 2 kDa) purchased from Merck (Darmstadt, Germany). Deionized water was purified using a water purification system by Millipore (Burlington, Massachusetts, USA), with a minimum resistivity of 18.0 M Ω cm. All grafting reactions were performed under dry and inert conditions (argon atmosphere), using Schlenk technique and custom-made glassware (**Figure S1**).

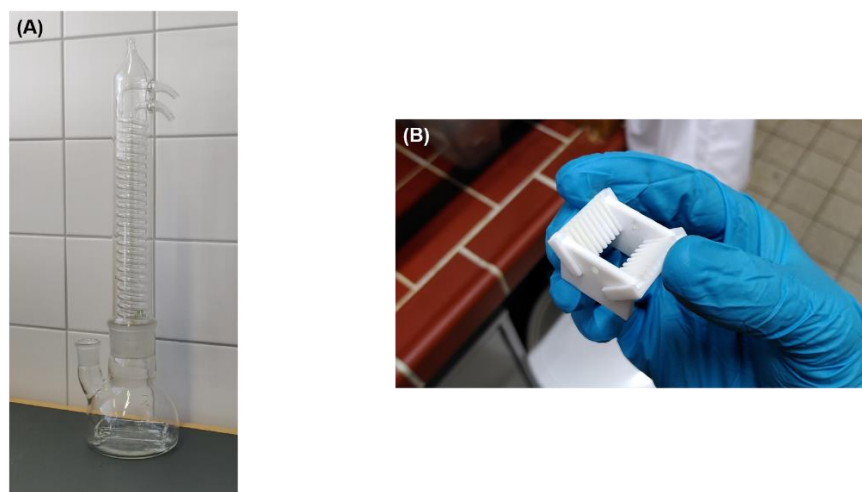


Figure S1. (A) Custom-made glassware for the incubation of the substrates with glycidol. The glassware was fabricated in such a manner that it could withstand the high vacuum (1×10^{-3} bar)

conditions that were required for the drying process of the flask. The cooler was necessary because glycidol tends to evaporate at elevated temperatures ($> 100\text{ }^{\circ}\text{C}$). The glass flask contained a glass rack at the bottom, which was used for the placement of the substrate holders. (B) A picture of one of the custom-made Teflon substrate holders that were used to place the (MI-dPG-coated) substrates into the reaction flask.

1.1.1. Static Water Contact Angle Measurements

Static water contact angle (CA) measurements were performed by applying a Dataphysics Instruments GmbH (Filderstadt, Germany) OCA 20 contact-angle measure device, according to the sessile drop method. The OCA 20 system was equipped with a six-fold zoom lens with integrated fine focus ($\pm 6\text{ mm}$) and a high light-transmitting-capacity CCD-camera, with a resolution of max 768×576 pixels. The used video system was a high performance imaging processing system, with a 132 Mbytes/s data transfer rate, and a digitizing speed up to 50 images/s. Image processing was performed by applying SCA 202 software also by Dataphysics Instruments GmbH.

1.1.2. Scanning Electron Microscopy

The surface morphology was investigated using a field emission scanning electron microscope (FE-SEM) model SU8030 by Hitachi (Chiyoda, Japan), at an accelerating voltage (V_{ac}) of 20 kV, a current of $15\text{ }\mu\text{A}$, and a working distance of 8.5 inches. The substrates were sputtered with a 5

nm conductive gold layer prior to the SEM measurements, using a CCU-010 sputter machine by Safematic GmbH (Bad Ragaz, Switzerland).

1.1.3. X-Ray Photoelectron Spectroscopy

X-ray photoelectron spectroscopy (XPS) spectra were recorded on a Kratos (Manchester, UK) Axis Ultra DLD spectrometer, equipped with a monochromatic Al K α X-ray source. The spectra were measured in normal emission, and a source-to-sample angle 60° was used. All spectra were recorded utilizing the fixed analyzer transmission (FAT) mode. The binding energy scale of the instrument was calibrated, following a technical procedure provided by Kratos Analytical Ltd (calibration was performed according to ISO 15472). The spectra were recorded utilizing the instrument's slot and hybrid lens modes. An analysis area of approximately a 300 μ m x 700 μ m was investigated; charge neutralization was applied. For quantification, the survey spectra were measured with a pass energy of 80 electron volt (eV), and the spectra were quantified utilizing the empirical sensitivity factors that were provided by KRATOS (the sensitivity factors were corrected with the transmission function of the spectrometer).

The high-resolution XPS spectra were measured with a pass energy of 20 eV, and the respective data were processed using UNIFIT spectrum processing software.^[1] For fitting, a Shirley background and a Gaussian/Lorentzian sum function (peak shape model GL (30)) were used. If not denoted otherwise, the L-G mixing component was set to 0.35 for all peaks. In case of the C1s spectra, peak fitting was performed in such a manner that all residual structures were

removed, and all binding energies were calibrated to the signal observed for the aliphatic C–C bond component (observed at 248.8 eV).

1.1.4. MI-dPG Synthesis

Dendritic polyglycerol (dPG) with M_n : 12,000 and M_w : 16,000 was polymerized in a one-step ring-opening anionic polymerization, as described in earlier work by Sunder et al.^[2] The amine-functionalized dPG (dPG–NH₂) was produced by mesylation, azidation, and subsequent Staudinger reduction of the introduced azides, according to procedures that were earlier published by our group.^[3] The dPG–NH₂ (4 g, 0.38 mmol) was dissolved in MeOH (100 ml), and 10% HCl-solution was added until a neutral pH was obtained. Subsequently, an aqueous buffer solution of 2-(N-morpholino) ethane sulfonic acid (MES) (0.1 M, pH: 4.8) was added, so that a 1:1 (V:V) ratio of MeOH to buffer was obtained. Next, 3,4-dihydroxy-hydrocinnamic acid (DHHA) (20 g, 110 mmol, 2 equivalent respectively to 100% of the –NH₂ groups), 1-ethyl-3-(3-dimethylamino)propyl)carboiimide (21 g, 110 mmol, 2.0 equivalent respective to 100% of the –NH₂ groups) were added, and the resulting reaction mixture was stirred for 16 h at room temperature. The reaction mixture was then purified by dialysis in MeOH. In order to increase product stability (i.e., to prevent polymerization), 37% HCl-solution was added to the dialysis-solution (1 drop per gram of product). The pure product was obtained upon removal of the solvent by means of rotary evaporation. The product was stored under argon atmosphere at -20 °C.

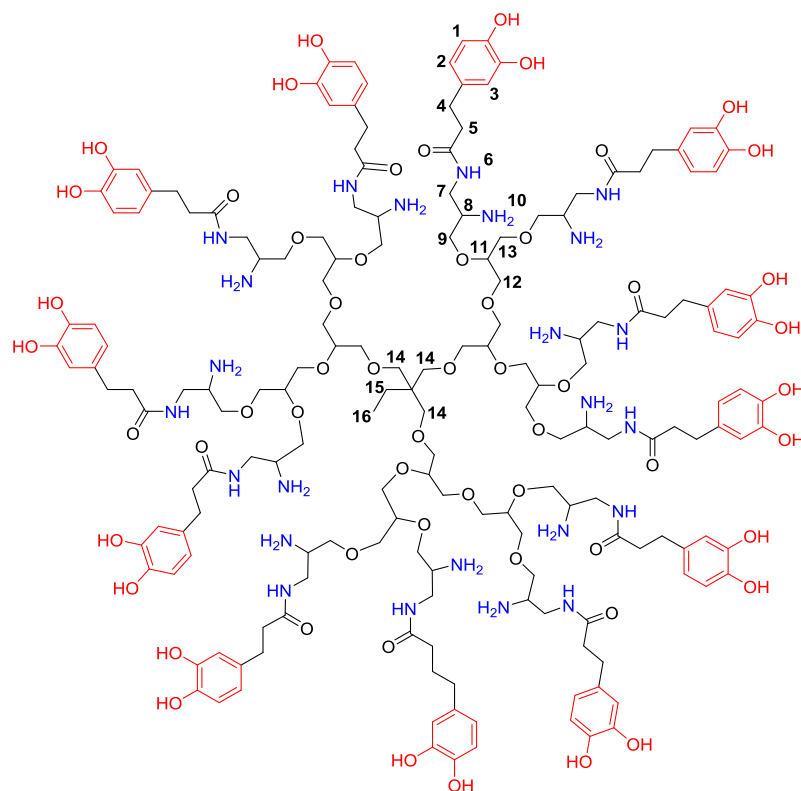


Figure S2. The molecular structure of MI-dPG. The depicted figure is an idealized dendrimer. The dPG-backbone structure shown in black varies with the molecular size of the MI-dPG and also contains unfunctionalized –OH moieties, resulting from chain termination during the polymerization process.

^1H NMR (500 MHz; CD_3OD): δ = 6.68-6.53 (**1-3**, m, aromatic protons); 4.21-3.02 (**7-14**, m, dPG-backbone); 2.74 (**5**, m, $-\text{RCOCH}_2\text{CH}_2\text{CR}-$); 2.44 (**4**, m, $-\text{COCH}_2\text{CH}_2\text{R}-$).^[4]

^{13}C NMR (700 MHz; CD_3OD): δ = 175.19, 174.27, and 172.13 (carboxylic carbons); 148.46-115.47 (aromatic carbons); 78.32-51.19 (dPG-backbone carbons); 37.532 and 35.582 ($-\text{COCH}_2\text{CH}_2\text{C}-$); 30.589 and 30.007 ($-\text{COCH}_2\text{CH}_2\text{C}-$) ppm.^[5]

1.2. SURFACE CHEMISTRY

1.2.1. Coating glass with TiO₂ via Physical Vapor Deposition

Glass microscope slides (76 mm x 26 mm, thickness 1 mm) purchased from VWR International (Radnor, Pennsylvania, USA) were coated with a transparent titanium dioxide (TiO₂) layer (ca. 30 nm) by means of physical vapor deposition (PVD). The TiO₂ coatings were prepared using radio frequency (13.56 MHz) reactive sputtering. Oxygen 5.0 and argon 4.6 purchased from Linde plc (Munich, Germany), and a titanium target (99.9 % purity) purchased from Sindlhauser Materials GmbH (Kempten, Germany) were used as source materials. The sputtering chamber (50 cm x 50 cm x 50 cm) was evacuated to a base pressure of 1×10^{-5} mbar. Subsequently, the substrates were plasma cleaned with oxygen (60 standard cubic centimeter per minute (sccm)) and argon (60 sccm) for 5 min (sputtering power: 2380 W). Without venting the chamber, the target was sputtered using an Ar-flux (120 sscm, sputter power: 2380 W). After the sputter plasma showed a blue color, an additional 9 sccm of oxygen was added to the chamber. The blue color indicated metallic titanium on the surface of the target, i.e., the absence of a TiO₂-layer. After a reactive sputtering time of 10 min, a 25 nm thick TiO₂-coating was obtained on the substrates. To get fully oxidized TiO₂, the distance between target and substrate was maximized (58 cm).

1.2.2. PDMS Spin Coating

Glass microscope slides (76 mm x 26 mm, thickness 1 mm) purchased from VWR International (Radnor, Pennsylvania, USA) were spin coated with a solution of PDMS in xylol (1 wt%). The glass slides (cut in ca. 1 x 1 cm) were spin coated at 3,000 rpm for 1 min. Spin coating was performed using a WS-650Mz-23NPPB spin coater by Laurell Technologies corporation (North Wales, Pennsylvania, USA).

1.2.3. MI-dPG Coating

TiO₂-coated glass substrates were cleaned by ultrasonic treatment in EtOH for 10 min, prior the coating procedure. The cleaned surfaces were then immersed in a solution of MI-dPG (4 mg, 1.33×10^{-4} mmol) in MeOH (2 ml) to which an aqueous solution of 3-(*N*-morpholino)propane sulfonic acid (MOPS) buffer (2 ml, 0.1 M, pH: 8.5) was added, initiating the polymerization reaction of MI-dPG. The surfaces were immersed in the polymerizing solution for 10 min (immersion depth ca 1 cm), after which they were removed from the solution and thoroughly rinsed with EtOH. Subsequently, the substrates were dried under a N₂-flow and placed in a custom glass flask (**Figure S1**) at 110 °C under high vacuum conditions (1×10^{-3} bar) for > 10 h. The PDMS-spin-coated substrates were functionalized with MI-dPG according to the same procedure.

1.2.4. dPG Grafting

Prior to the grafting reaction, glycidol was dried overnight in a pre-dried Schlenk-flask containing molecular sieve (type 562 C, pore size 3 Å) by Carl Roth GmbH (Karlsruhe, Germany). Additionally, the (MI-dPG-coated) substrates were dried overnight at 110 °C under high vacuum conditions (1×10^{-3} bar) using custom glassware (**Figure S1**). The flask was removed from the oil bath and was cooled down to room temperature. The flask was then flushed with argon, and subsequently glycidol was added to the flask under argon backflow. Next, the flask was placed back in the oil bath at 80 °C, 100 °C, or 120 °C for 30 min, 1 h, 3 h, or 24 h, allowing the grafting of dendritic polyglycerol (dPG) from the surface. After the grafting reaction, the substrates were removed from the system, thoroughly rinsed with EtOH (3x), and subsequently placed in a beaker glass containing in EtOH for > 10 h. Next, the substrates were dried under N₂ flow and dried at 50 °C for 1 h prior to any further measurements.

1.3. BIOLOGICAL ASSAYS

1.3.1. LIVE/DEAD Staining of A549 and DF-1 Cells

Human adenocarcinoma cells (A549 cells) and chicken fibroblast cells (DF-1 cells) were maintained as a monolayer culture in tissue culture polystyrene (TCPS) petri dishes containing Dulbecco's Modified Eagle's Medium (DMEM) supplemented with fetal bovine serum (FBS) (10 v%), streptomycin (100 mg/ml), and penicillin (100 units/ml). The cell lines were cultured under 5% CO₂ at 37 °C, using a laboratory CO₂ incubator by Heraeus Holding GmbH (Hanau, Germany). MI-dPG coated substrates were prepared according to the procedure described in

Section 1.2.3. of this document. Subsequently, the samples were sterilized with EtOH (75 vol% in Milli-Q) for 10 min and washed with cell culture medium before the seeding. The A549 cells were seeded at a concentration of 1×10^6 cells/mL. The DF-1 cells were seeded at a concentration of 5×10^6 cells/mL. After 24 h of culturing, the cells were stained utilizing a commercially available LIVE/DEAD™ Viability/Cytotoxicity Kit (Order No: L3224) by Thermo Fisher Scientific Inc. (Waltham, Massachusetts, USA) and visualized using AxioObserver Z.1 microscope by the Carl Zeiss AG (Oberkochen, Germany). Zen blue software (also provided by the Carl Zeiss AG) was applied for image capturing.

1.3.2. Automated LIVE/DEAD™ Quantification

Automatic image analysis was performed with the Java-based image processing program "ImageJ" developed by the Laboratory for Optical and Computational Instrumentation of the University of Wisconsin (Madison, Wisconsin, USA).^[6] Cell recognition was achieved via distinctive assessment of fluorescence signals from live and dead cells. First, the cells were separated from the background utilizing the "subtract background" function of "ImageJ". In this process, a rolling ball radius of 50 pixels was chosen. The cells were separated from the background by thresholding the fluorescence value of the 16-bit images (threshold_{Live}: 1510, threshold_{Dead}: 150). After binarization, cell clusters were segmented utilizing a "watershed algorithm" for the separation of different objects in an image (coefficient: 0.1). Subsequently, the particle analyzer function of ImageJ was utilized for cell quantification and morphology analysis. To avoid counting single pixels or cell fragments, only objects above a specific size were analyzed (i.e., only objects bigger than 10 pixels were analyzed). Finally, the results were

manually evaluated by comparing the outlines of the analyzed particles with the original fluorescence images. Insufficiently segmented cell clusters were manually recounted.

2. RESULTS

2.1. CA Results

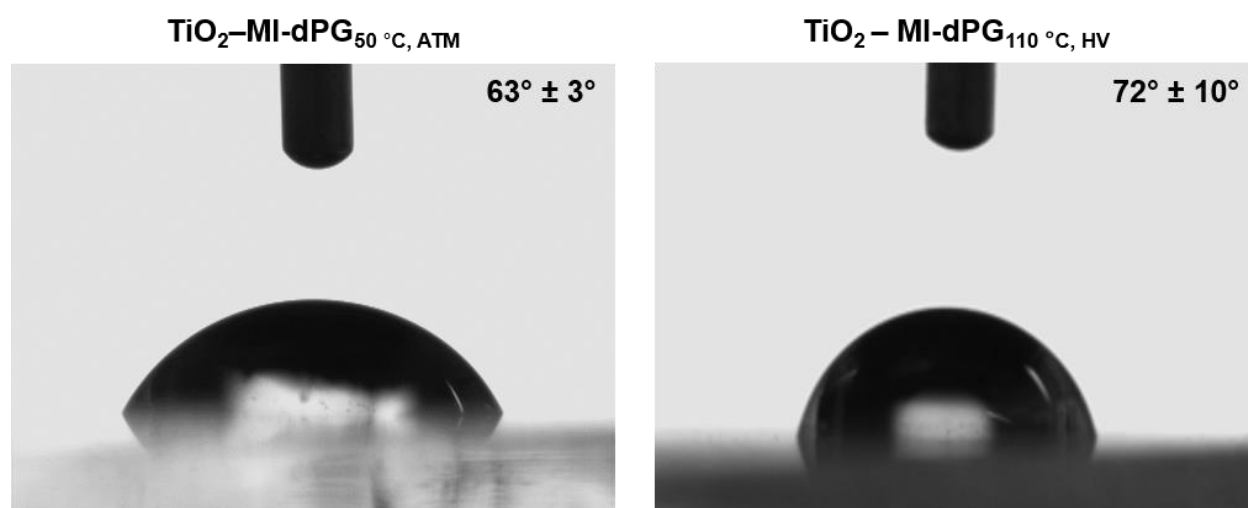


Figure S3. CA Pictures of TiO₂-MI-dPG_{50 °C, ATM} (left) and TiO₂-MI-dPG_{110 °C, HV} (right). An increase in the CA was observed after drying of the coating at elevated temperatures under high vacuum conditions.

Table S1. CA values for TiO₂–MI-dPG_{50 °C, ATM} and TiO₂–MI-dPG_{110 °C, HV}.

<i>S</i> ^A	TiO₂–MI-dPG_{50 °C, ATM}			Mean (μ)	STDV^B (σ)
<i>I</i>	65.8°	64.1°	64.5°		
<i>II</i>	59.6°	63.2°	64.6°	62.6°	2.9°
<i>III</i>	56.1°	61.4°	64.0°		
TiO₂–MI-dPG_{110 °C, HV}					
<i>I</i>	60.1°	52.1°	62.6°		
<i>II</i>	79.6°	77.6°	79.8°	71.9°	10.0°
<i>III</i>	79.1°	78.3°	78.2°		

Note for A, S = Substrate. Note for B, STDV = Standard deviation from the mean.

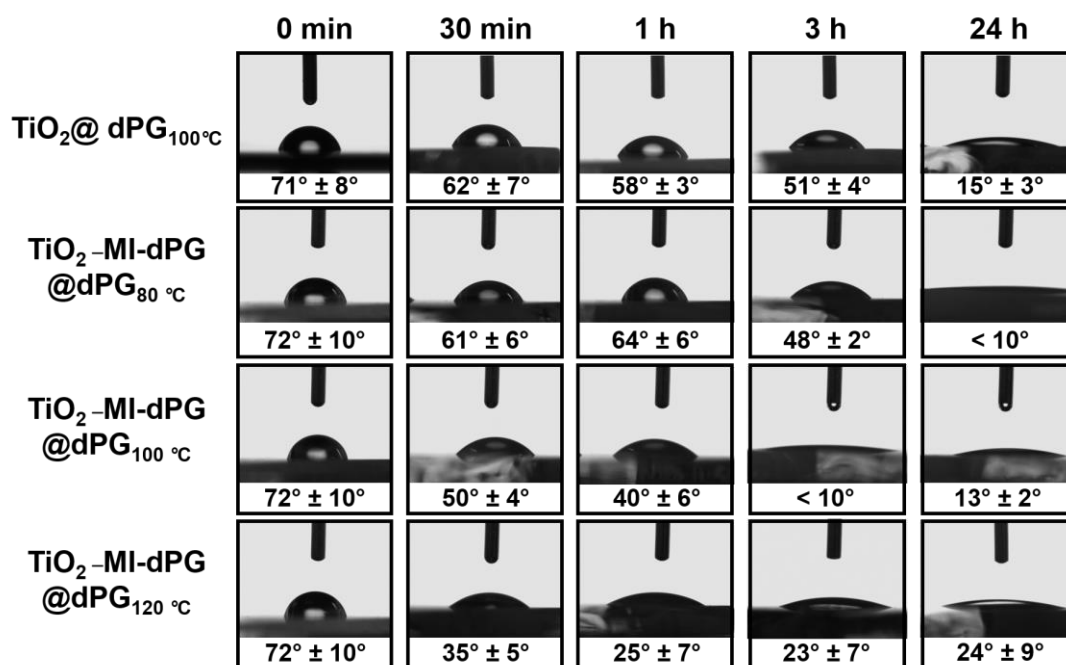


Figure S4. The images and the average CA values obtained for $\text{TiO}_2@ \text{dPG}$ and $\text{TiO}_2\text{--MI-dPG}@ \text{dPG}$ at various dPG grafting times and temperatures.

Table S2. CA values for TiO_2 and $\text{TiO}_2\text{--MI-dPG}$ after dPG grafting at various times and temperatures.

S^A		Bare TiO_2	Mean (μ)	STDV ^B (σ)
<i>I</i>	72.4°	69.0°	79.5°	
<i>II</i>	80.1°	73.5°	78.3°	71.9° 6.1°
<i>III</i>	67.5°	63.9°	63.0°	

TiO₂@dPG_{30 min, 100 °C}					
<i>I</i>	60.2°	65.2°	62.6°		
<i>II</i>	66.9°	64.7°	64.2°	62.3°	7.3°
<i>III</i>	42.6°	68.0°	66.2°		
TiO₂@dPG_{1 h, 100 °C}					
<i>I</i>	61.2°	58.0 °	55.7°		
<i>II</i>	55.3°	56.3°	59.0°	57.7°	2.5°
<i>III</i>	53.6°	58.4°	61.4°		
TiO₂@dPG_{3 h, 100 °C}					
<i>I</i>	53.5°	54.2°	52.4°		
<i>II</i>	54.2°	41.2°	51.2°	51.4°	3.9°
<i>III</i>	54.2°	51.6°	50.0°		
TiO₂@dPG_{24 h, 100 °C}					
<i>I</i>	17.0°	12.2°	11.5°		
<i>II</i>	16.6°	15.1°	16.7°	15.1°	2.5°
<i>III</i>	11.4°	17.3°	18.2°		

TiO₂–MI-dPG					
<i>I</i>	60.1°	52.1°	62.6°		
<i>II</i>	79.6°	77.6°	79.8°	71.9°	10.0°
<i>III</i>	79.1°	78.3°	78.2°		
TiO₂–MI-dPG@dPG_{30 min}, 80 °C					
<i>I</i>	63.2°	47.0°	62.2°		
<i>II</i>	63.7°	62.1°	58.4°	61.3°	5.6°
<i>III</i>	63.3°	67.9°	64.0°		
TiO₂–MI-dPG@dPG_{1 h}, 80 °C					
<i>I</i>	72.0°	69.1°	70.8°		
<i>II</i>	54.4°	55.8°	57.3°	64.0°	6.2°
<i>III</i>	66.4°	63.9°	66.3°		
TiO₂–MI-dPG@dPG_{3 h}, 80 °C					
<i>I</i>	50.7°	46.9°	49.6°		
<i>II</i>	47.6°	44.8°	44.8°	47.8°	1.9°
<i>III</i>	48.1°	49.1°	48.6°		

TiO₂–MI-dPG@dPG_{24 h, 80 °C}					
<i>I</i>	9.3°	5.9°	< 10°		
<i>II</i>	3.1°	< 10°	< 10°	< 10°	N.A.
<i>III</i>	4.5°	8.8°	< 10°		
TiO₂–MI-dPG@dPG_{30 min, 100 °C}					
<i>I</i>	57.8°	54.8°	47.4°		
<i>II</i>	48.9°	46.5°	53.7°	50.1°	4.0°
<i>III</i>	48.0°	46.2°	47.4°		
TiO₂–MI-dPG@dPG_{1 h, 100 °C}					
<i>I</i>	44.2°	44.4°	42.5°		
<i>II</i>	39.1°	47.5°	33.3°	40.1°	5.6°
<i>III</i>	42.3°	39.1°	28.8°		
TiO₂–MI-dPG@dPG_{3 h, 100 °C}					
<i>I</i>	< 10°	< 10°	10.7°		
<i>II</i>	< 10°	< 10°	< 10°	< 10°	N.A.
<i>III</i>	< 10°	< 10°	< 10°		

TiO₂–MI-dPG@dPG_{24 h, 100 °C}					
<i>I</i>	12.1°	12.5°	13.3°		
<i>II</i>	< 10°	13.8°	11.6°	12.5°	1.5°
<i>III</i>	13.4°	14.7°	11.9°		
TiO₂–MI-dPG@dPG_{30 min, 120 °C}					
<i>I</i>	32.8°	40.3°	34.6°		
<i>II</i>	28.7°	26.6°	39.4°	35.0°	4.5°
<i>III</i>	36.3°	36.9°	38.9°		
TiO₂–MI-dPG@dPG_{1 h, 120 °C}					
<i>I</i>	33.5°	14.9°	27.3°		
<i>II</i>	31.7°	21.6°	33.6°	25.4°	6.5°
<i>III</i>	19.3°	27.4°	19.0°		
TiO₂–MI-dPG@dPG_{3 h, 120 °C}					
<i>I</i>	30.7°	20.1°	14.6°		
<i>II</i>	22.4°	13.7°	15.3°	23.1°	7.2°
<i>III</i>	26.9°	29.9°	34.1°		

TiO₂–MI-dPG@dPG_{24 h, 120 °C}					
<i>I</i>	24.2°	11.8°	13.7°		
<i>II</i>	37.8°	24.3°	15.9°	24.1°	9.2°
<i>III</i>	22.5°	27.5°	39.6°		
Bare PDMS					
<i>I</i>	111.5°	112.3°	110.8°		
<i>II</i>	102.6°	113.9°	106.4°	108.1°	3.8°
<i>III</i>	106.0°	103.7°	105.8°		

Note for A, S = Substrate. Note for B, STDV = Standard deviation from the mean.

2.2. XPS Results

Table S3. Highly resolved C1s spectra for TiO₂, TiO₂–MI-dPG₅₀ °C, ATM, TiO₂–MI-dPG₁₁₀ °C, HV as determined by XPS.

<i>Substrate</i>	<i>Spectrum</i>	<i>Binding energy</i>	<i>L-G Mixing</i>	<i>FWHM</i>	<i>Chemical state</i>	<i>Rel. Area</i>
TiO₂	C 1s	284.8	0.35	1.4	C–C	0.78
		286.1	0.35	1.0	C–O	0.15
		288.2	0.35	1.0	C=O	0.07
TiO₂– MI-dPG₅₀ °C, ATM	C1s	284.8	0.35	1.2	C–C	0.40
		286.3	0.35	1.1	C–O	0.54
		288.1	0.35	1.1	C=O	0.06
TiO₂– MI-dPG₁₁₀ °C, HV	C1s	284.8	0.35	1.2	C–C	0.44
		286.2	0.35	1.1	C–O	0.48
		288.1	0.35	1.1	C=O	0.08
		289.2	0.35	1.1	O–C=O	0.00

Fitting parameters and the relative areas for C1s component peaks at various binding energies in XPS. The values reported for the C–O component include the C–N component resulting from peak overlap.

Table S4. The C–O/C–C component peak area ratios for TiO₂, TiO₂–MI-dPG_{50 °C, ATM}, and TiO₂–MI-dPG_{110 °C, HV} as determined by XPS.

<i>Substrate</i>	<i>C–O/C–C</i>
TiO₂	0.19
TiO₂–MI-dPG_{50 °C, ATM}	1.35
TiO₂–MI-dPG_{110 °C, HV}	1.09

The C–O/C–C component peak area ratios were calculated by dividing the relative area of the peak fitted at ~286.5 eV (for the C–O component) by the relative area for the peak fitted at ~285.0 eV (for the C–C and C=C components). The values reported for the C–O component include the C–N component resulting from peak overlap.

Table S5. Atomic C-, O-, N- and Ti-fractions of TiO₂, TiO₂-MI-dPG_{50 °C, ATM} and TiO₂-MI-dPG_{110 °C, HV} as determined by XPS.

<i>Substrate</i>	<i>C(at.%)^A</i>	<i>O (at.%)^A</i>	<i>N (at.%)^A</i>	<i>Ti (at.%)^A</i>
TiO₂	22.3	52.3	0.6	12.9
TiO₂-MI-dPG_{50 °C, ATM}	67.4	23.3	7.3	0.6
TiO₂-MI-dPG_{110 °C, HV}	66.6	24.2	5.8	0.8

The elemental contents were extracted from the respective survey spectra (**Figure S9** of the appendix). Note for A, at.% = atomic percentage.

Table S6. Highly resolved C1s spectra for TiO₂ and TiO₂-MI-dPG after dPG grafting at varying reaction times and temperatures as determined by XPS.

<i>Substrate</i>	<i>Spectrum</i>	<i>Binding energy</i>	<i>L-G Mixing</i>	<i>FWHM</i>	<i>Chemical state</i>	<i>Rel. Area</i>
TiO₂	C 1s	284.8	0.35	1.4	C-C	0.78
		286.1	0.35	1.0	C-O	0.15
		288.2	0.35	1.0	C=O	0.07

	C1s	284.8	0.35	1.2	C–C	0.41
TiO₂		286.2	0.35	1.2	C–O	0.50
@dPG _{30 min} , 100 °C		288.1	0.35	1.1	C=O	0.05
		289.0	0.35	1.1	O–C=O	0.04
	C1s	284.8	0.35	1.2	C–C	0.36
TiO₂		286.2	0.35	1.2	C–O	0.58
@dPG _{1 h} , 100 °C		288.1	0.35	1.1	C=O	0.04
		289.0	0.35	1.1	O–C=O	0.02
	C1s	284.8	0.35	1.1	C–C	0.31
TiO₂		286.0	0.35	1.3	C–O	0.60
@dPG _{3 h} , 100 °C		287.8	0.35	1.1	C=O	0.03
		288.8	0.35	1.1	O–C=O	0.06
	C1s	284.8	0.35	1.0	C–C	0.17
TiO₂		286.3	0.35	1.1	C–O	0.77
@dPG _{24 h} , 100 °C		287.8	0.35	1.1	C=O	0.04
		289.1	0.35	1.1	O–C=O	0.02

	C1s	284.8	0.35	1.2	C–C	0.34
TiO₂ –		286.2	0.35	1.1	C–O	0.58
MI-dPG						
@dPG_{30 min}, 80 °C		288.0	0.35	1.1	C=O	0.08
		289.1	0.35	1.1	O–C=O	0.01
	C1s	284.8	0.35	1.3	C–C	0.34
TiO₂ –		286.2	0.35	1.1	C–O	0.56
MI-dPG						
@dPG_{1 h}, 80 °C		288.0	0.35	1.1	C=O	0.04
		283.6	0.35	1.1	Charge ^A	0.06
	C1s	284.8	0.35	1.2	C–C	0.28
TiO₂ –		286.2	0.35	1.2	C–O	0.68
MI-dPG						
@dPG_{3 h}, 80 °C		288.1	0.35	1.2	C=O	0.03
		283.9	0.35	1.2	Charge ^A	0.06
	C1s	284.8	0.35	1.0	C–C	0.29
TiO₂ –		286.3	0.35	1.1	C–O	0.67
MI-dPG						
@dPG_{24 h}, 80 °C		287.8	0.35	1.1	C=O	0.03
		289.0	0.35	1.1	O–C=O	0.01

	C1s	284.8	0.35	1.0	C–C	0.24
TiO₂–		286.3	0.35	1.1	C–O	0.70
MI-dPG						
@dPG_{30 min, 100 °C}		287.9	0.35	1.1	C=O	0.05
		289.0	0.35	1.1	O–C=O	0.01
	C1s	284.8	0.35	1.0	C–C	0.18
TiO₂–		286.3	0.35	1.1	C–O	0.77
MI-dPG						
@dPG_{1 h, 100 °C}		287.9	0.35	1.1	C=O	0.04
		289.1	0.35	1.1	O–C=O	0.01
	C1s	284.8	0.35	1.0	C–C	0.16
TiO₂–		286.3	0.35	1.1	C–O	0.80
MI-dPG						
@dPG_{3 h, 100 °C}		287.9	0.35	1.1	C=O	0.04
		289.0	0.35	1.1	O–C=O	0.01
	C1s	284.8	0.35	1.0	C–C	0.09
TiO₂–		286.4	0.35	1.1	C–O	0.86
MI-dPG						
@dPG_{24 h, 100 °C}		287.8	0.35	1.1	C=O	0.04
		289.1	0.35	1.1	O–C=O	0.01

	C1s	284.8	0.35	1.0	C–C	0.22
TiO₂–		286.3	0.35	1.1	C–O	0.73
MI-dPG						
@dPG_{30 min}, 120 °C		287.9	0.35	1.1	C=O	0.04
		289.0	0.35	1.1	O–C=O	0.01
	C1s	284.8	0.35	1.0	C–C	0.20
TiO₂–		286.3	0.35	1.1	C–O	0.75
MI-dPG						
@dPG_{1 h}, 120 °C		287.9	0.35	1.1	C=O	0.04
		289.0	0.35	1.1	O–C=O	0.01
	C1s	284.8	0.35	1.0	C–C	0.18
TiO₂–		286.3	0.35	1.1	C–O	0.78
MI-dPG						
@dPG_{3 h}, 120 °C		287.8	0.35	1.1	C=O	0.04
		289.1	0.35	1.1	O–C=O	0.01
	C1s	284.8	0.35	1.0	C–C	0.06
TiO₂–		286.4	0.35	1.1	C–O	0.90
MI-dPG						
@dPG_{24 h}, 120 °C		287.8	0.35	1.1	C=O	0.03
		289.1	0.35	1.1	O–C=O	0.01

Fitting parameters and the relative areas for C1s component peaks at various binding energies in XPS. The values reported for the C–O component include the C–N component resulting from peak overlap. Note for A, during XPS-measurements the substrates might electrostatically charge, due to the removal of electrons in proximity of the atomic nuclei. This charge is automatically corrected via charge correction procedures, but might still lead to observable peaks in the highly resolved C1s spectra.

Table S7. The C–O/C–C component peak area ratios for TiO₂, TiO₂–MI–dPG with dPG grafting at varying reaction times and temperatures as determined by XPS

<i>Substrate</i>	<i>C–O/C–C</i>
TiO₂	0.19
TiO₂@dPG_{30 min, 100 °C}	1.22
TiO₂@dPG_{1 h, 100 °C}	1.61
TiO₂@dPG_{3 h, 100 °C}	1.94
TiO₂@dPG_{24 h, 100 °C}	4.53
TiO₂–MI–dPG@dPG_{30 min, 80 °C}	1.71
TiO₂–MI–dPG@dPG_{1 h, 80 °C}	1.65
TiO₂–MI–dPG@dPG_{3 h, 80 °C}	2.43

TiO₂–MI-dPG@dPG_{24 h, 80 °C}	2.31
TiO₂–MI-dPG@dPG_{30 min, 100 °C}	2.92
TiO₂–MI-dPG@dPG_{1 h, 100 °C}	4.28
TiO₂–MI-dPG@dPG_{3 h, 100 °C}	5.00
TiO₂–MI-dPG@dPG_{24 h, 100 °C}	9.56
TiO₂–MI-dPG@dPG_{30 min, 120 °C}	3.32
TiO₂–MI-dPG@dPG_{1 h, 120 °C}	3.75
TiO₂–MI-dPG@dPG_{3 h, 120 °C}	4.33
TiO₂–MI-dPG@dPG_{24 h, 120 °C}	15.00

The obtained ratios were calculated by dividing the relative area of the peak fitted at ~286.5 eV (for C–O component) by the relative area for the peak fitted at ~285.0 eV (C–C and C=C components). The values reported for the C–O component include the C–N component, resulting from peak overlap.

Table S8. The atomic C-, O-, N-, and Ti-fractions for TiO₂, TiO₂–MI-dPG after dPG grafting at varying reaction times and temperatures as determined by XPS.

<i>Substrate</i>	<i>C(at.%)</i>	<i>O (at.%)</i>	<i>N (at.%)</i>	<i>Ti (at.%)</i>
TiO₂	22.3	52.3	0.6	12.9
TiO₂@dPG_{30 min, 100 °C}	30.5	51.6	0.3	16.3
TiO₂@dPG_{1 h, 100 °C}	29.3	52.6	0.2	15.6
TiO₂@dPG_{3 h, 100 °C}	36.8	49.3	0.4	12.4
TiO₂@dPG_{24 h, 100 °C}	59.8	37.7	0	1.8
TiO₂–MI-dPG	66.6	24.2	5.8	0.8
TiO₂– MI-dPG@dPG_{30 min, 80 °C}	66.7	27.2	5.0	0.4
TiO₂– MI-dPG@dPG_{1 h, 80 °C}	68.2	27.3	3.6	0.2
TiO₂– MI-dPG@dPG_{3 h, 80 °C}	64.9	32.2	2.2	0.5
TiO₂– MI-dPG@dPG_{24 h, 80 °C}	70.2	29.2	0.5	0.0

TiO₂– MI-dPG@dPG_{30 min, 100 °C}	66.1	30.6	2.9	0.0
TiO₂– MI-dPG@dPG_{1 h, 100 °C}	64.9	33.3	1.5	0.1
TiO₂– MI-dPG@dPG_{3 h, 100 °C}	65.3	33.8	0.8	0.0
TiO₂– MI-dPG@dPG_{24 h, 100 °C}	64.0	35.8	0.0	0.0
TiO₂– MI-dPG@dPG_{30 min, 120 °C}	65.5	32.3	1.7	0.3
TiO₂– MI-dPG@dPG_{1 h, 120 °C}	66.3	32.1	1.0	0.0
TiO₂– MI-dPG@dPG_{3 h, 120 °C}	66.9	32.3	0.4	0.0
TiO₂– MI-dPG@dPG_{24 h, 120 °C}	62.7	36.9	0.2	0.0

The elemental contents were extracted from the C1s, O1s, N1s and Ti2p peaks of the respective survey spectra (**Figure S9, S10, and S11** of the appendix).

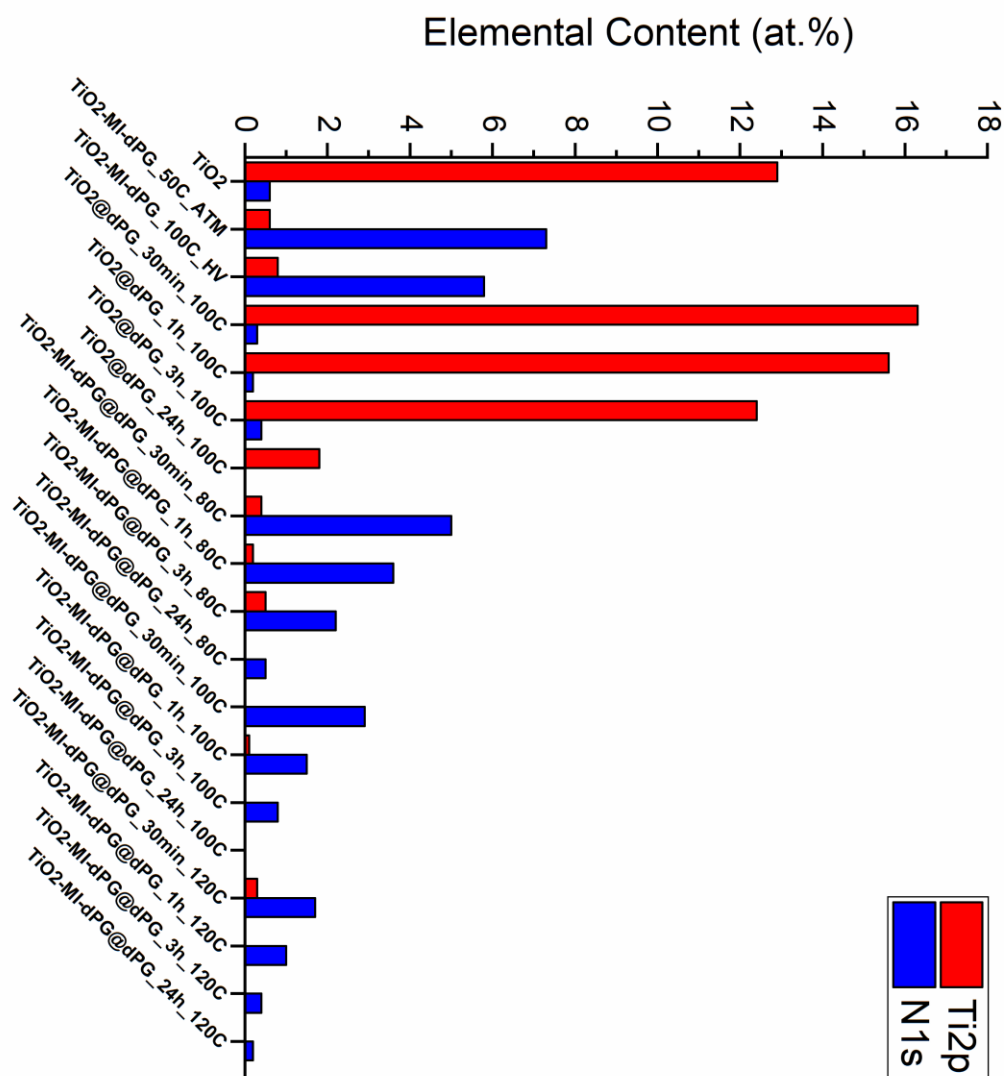


Figure S5. A graph showing the Ti2p and N1s elemental content (in at.%) for TiO₂ and TiO₂–MI–dPG after dPG grafting at varying reaction times and temperatures as determined by XPS. The elemental contents were extracted from the respective survey spectra (**Figures S9, S10** and **S11** of the appendix).

Table S9. Highly resolved C1s spectra for PDMS and PDMS–MI-dPG after dPG grafting at 100 °C for 3 h as determined by XPS.

<i>Substrate</i>	<i>Spectrum</i>	<i>Binding energy</i>	<i>L-G Mixing</i>	<i>FWHM</i>	<i>Interpretation</i>	<i>Rel. Area</i>
PDMS	C1s	284.8	0.35	1.1	Si–C	1.00
PDMS @dPG_{3 h, 100 °C}	C1s	284.8	0.35	1.0	Si–C	0.99
		286.3	0.35	1.0	C–O	0.01
PDMS – MI-dPG	C1s	284.8	0.35	1.0	Si–C & C–C	0.90
		286.4	0.35	1.0	C–O	0.09
		287.9	0.35	1.0	C=O	0.01
PDMS – MI-dPG @dPG_{3 h, 100 °C}	C1s	284.8	0.35	1.1	Si–C & C–C	0.36
		286.6	0.35	1.0	C–O	0.63
		288.1	0.35	1.0	C=O	0.02

Fitting parameters and the relative areas for C1s component peaks at various binding energies in XPS. The values reported for the C–O component include the C–N component resulting from peak overlap.

Table S10. The C–O/(Si–C & C–C) component peak area ratios for PDMS and PDMS–MI-dPG after dPG grafting at 100 °C for 3 h determined from XPS.

<i>Substrate</i>	<i>C–O/(Si–C & C–C)</i>
PDMS	0.00
PDMS@dPG_{3 h, 100 °C}	0.01
PDMS–MI-dPG	0.10
PDMS–MI-dPG@dPG_{3 h, 100 °C}	1.75

The obtained ratios were calculated by dividing the relative area of the peak fitted at ~286.5 eV (for C–O component) by the relative area for the peak fitted at ~285.0 eV (Si–C, C–C and C=C components). The values reported for the C–O component include C–N component resulting from peak overlap.

Table S11. Atomic C, O, N and Si fractions of PDMS and PDMS–MI-dPG after dPG grafting at 100 °C for 3 h as determined by XPS.

<i>Substrate</i>	<i>C(at.%)</i>	<i>O (at.%)</i>	<i>N (at.%)</i>	<i>Si (at.%)</i>
PDMS	30.0	45.1	0.1	23.1
PDMS@dPG_{3 h, 100 °C}	51.5	25.5	0.3	22.7
PDMS–MI-dPG	61.5	23.6	1.4	13.5
PDMS–MI-dPG@dPG_{3 h, 100 °C}	60.2	32.1	0.3	7.5

The elemental contents were extracted from the C1s, O1s, N1s and Si2p peaks of the respective survey spectra (**Figure S11** of the appendix).

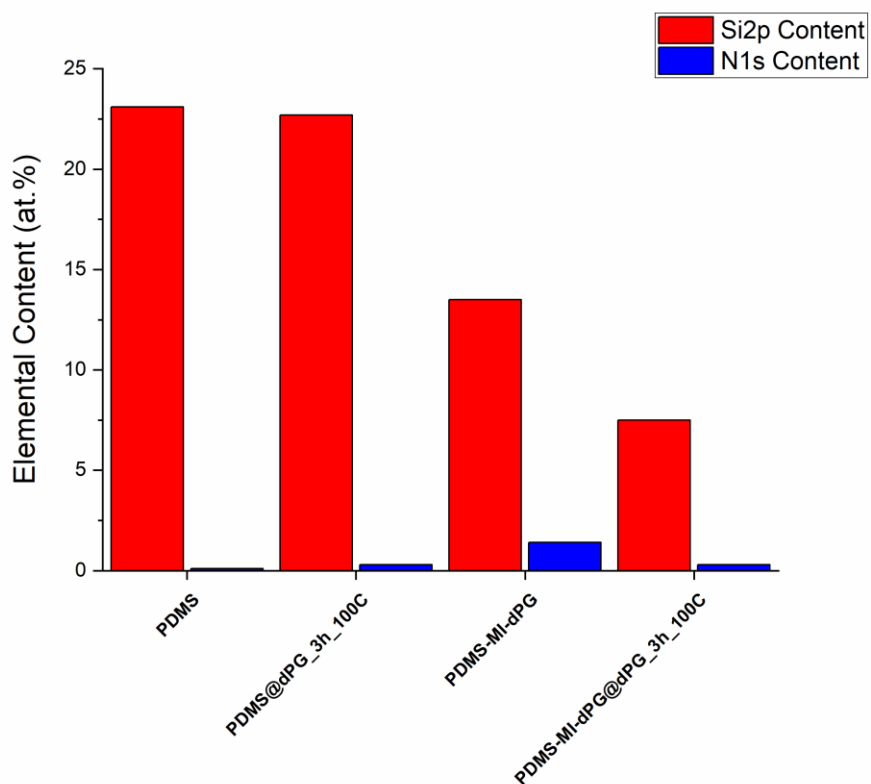


Figure S6. A graph showing the Si2p and N1s' elemental content for PDMS, PDMS@dPG_{3 h, 100 °C}, PDMS-MI-dPG, and PDMS-MI-dPG@dPG_{3 h, 100 °C} as determined by XPS. The elemental contents were extracted from the respective survey spectra (**Figure S11** of the appendix).

2.3. SEM Results

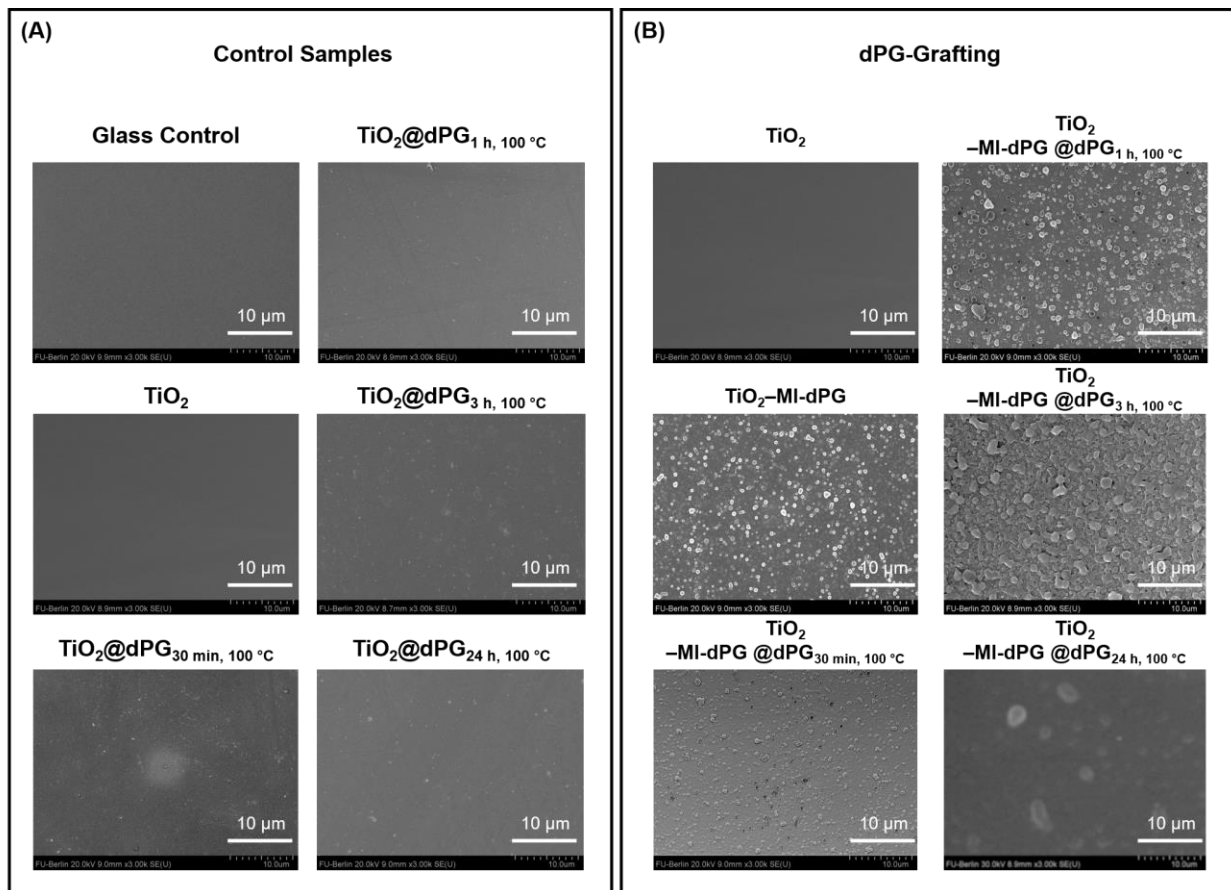


Figure S7. SEM Images showing the dPG grafting process from TiO₂ and TiO₂-MI-dPG at 100 °C. (A) For the bare TiO₂ substrate, only slight changes in the surface morphology were observed after incubation with glycidol under elevated temperatures. (B) In contrast, for the TiO₂-MI-dPG substrate, it was clearly observed that the roughness increased as a function of the reaction time resulting from the dPG grafting process.

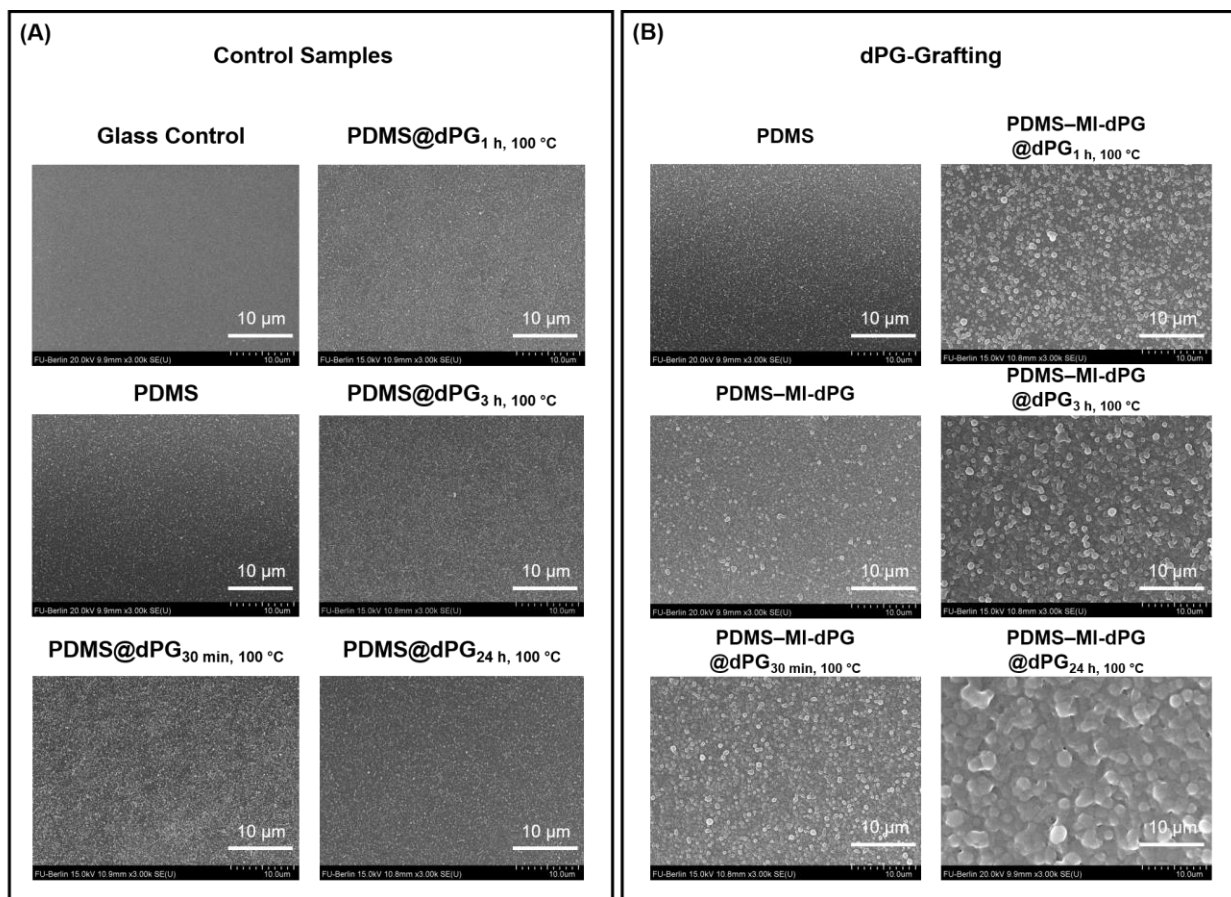


Figure S8. SEM Images showing the dPG grafting process from PDMS and PDMS–MI-dPG at 100 °C. (A) For the bare PDMS substrate, no obvious change in the morphology of the surface was observed after incubation with glycidol at elevated temperatures. (B) In contrast, for the PDMS–MI-dPG substrate, it was clearly observed that the surface roughness increased as a function of the reaction time resulting from the dPG grafting process.

2.4. Cell Viability Results

Table S12. Cell number and viability quantification via LIVE/DEAD™ staining.

<i>Substrate</i>		Live Cells		Dead Cells		Total Cell Number		Viability (%)	
		<i>A549</i>	<i>DF-1</i>	<i>A549</i>	<i>DF-1</i>	<i>A549</i>	<i>DF-1</i>	<i>A549</i>	<i>DF-1</i>
TCPS	I	962	356	3	1	965	357	0.99	1.00
TCPS	II	1044	371	7	2	1051	373	0.99	0.99
TCPS	III	1129	530	0	1	1129	531	1	1.00
TCPS	IV	1076	504	6	1	1082	505	0.99	1.00
TCPS	V	919	-	2	-	921	-	0.99	-
TiO ₂	I	1031	445	2	4	1033	449	0.99	0.99
TiO ₂	II	956	298	5	0	961	298	0.99	1.00
TiO ₂	III	1098	609	5	10	2003	619	0.99	0.98
TiO ₂	IV	1205	406	3	2	1208	408	0.99	1.00
TiO ₂ @dPG ^A	I	935	576	2	5	937	581	0.99	0.99
TiO ₂ @dPG ^A	II	1088	403	2	7	1090	409	0.99	0.98
TiO ₂ @dPG ^A	III	861	305	1	11	862	316	0.99	0.97

TiO₂@dPG^A	IV	855	384	9	10	864	394	0.99	0.98
TiO₂-MI-dPG	I	867	151	1	1	868	152	0.99	0.99
TiO₂-MI-dPG	II	840	153	0	13	840	166	1.00	0.92
TiO₂-MI-dPG	III	866	256	5	20	871	276	0.99	0.93
TiO₂-MI-dPG	IV	1110	309	9	4	1119	313	0.99	0.99
TiO₂-MI-dPG @dPG^A	I	6	2	0	7	6	9	1.00	0.22
TiO₂-MI-dPG @dPG^A	II	1	5	0	4	1	9	1.00	0.56
TiO₂-MI-dPG @dPG^A	III	4	20	0	7	4	27	1.00	0.74
TiO₂-MI-dPG @dPG^A	IV	3	11	0	2	3	13	1.00	0.85
PDMS	I	1233	482	5	5	1238	487	0.99	0.99
PDMS	II	1088	436	11	41	1099	477	0.99	0.91
PDMS	III	1123	516	2	4	1125	520	0.99	0.99
PDMS	IV	976	476	5	5	981	481	0.99	0.98
PDMS	V	922	306	7	0	929	306	0.99	1.00
PDMS@dPG^A	I	881	331	40	1	921	332	0.95	1.00
PDMS@dPG^A	II	188	380	17	6	205	386	0.92	0.98

PDMS@dPG^A	III	976	285	48	9	1024	294	0.95	0.97
PDMS@dPG^A	IV	851	556	49	3	900	559	0.95	0.99
PDMS@dPG^A	V	635	-	41	-	676	-	0.94	-
PDMS-MI-dPG	I	860	208	3	11	863	219	0.99	0.95
PDMS-MI-dPG	II	992	276	5	12	997	289	0.99	0.96
PDMS-MI-dPG	III	1186	363	3	17	1189	380	0.99	0.96
PDMS-MI-dPG	IV	1121	372	10	8	1131	380	0.99	0.98
PDMS-MI-dPG @dPG^A	I	2	0	0	0	2	0	1.00	0
PDMS-MI-dPG @dPG^A	II	6	0	0	0	6	0	1.00	0
PDMS-MI-dPG @dPG^A	III	8	0	0	0	8	0	1.00	0
PDMS-MI-dPG @dPG^A	IV	2	-	0	-	2	-	1.00	-

For the A549 cells the cell numbers were determined on a 920 μm x 720 μm surface, for DF-1 the cell numbers were determined on a 790 μm x 600 μm surface; the cell numbers per cm^2 as reported in the main text were calculated accordingly. Note for A, dPG grafting was performed for 3 h at 100 $^{\circ}\text{C}$.

3. LITERATURE

- [1] A. O. Fitton, J. Hill, D. E. Jane, R. Millar, *Synthesis* **1987**, 1987, 1140.
- [2] A. Sunder, R. Hanselmann, H. Frey, R. Mülhaupt, *Macromolecules* **1999**, 32, 4240.
- [3] S. Roller, H. Zhou, R. Haag, *Molecular Diversity* **2005**, 9, 305.
- [4] H. e. al., *ACS Applied Materials & Interfaces* **2016**, 8, 29117.
- [5] Q. Wei, K. Achazi, H. Liebe, A. Schulz, P.-L. M. Noeske, I. Grunwald, R. Haag, *Angewandte Chemie International Edition* **2014**, 53, 11650.
- [6] M. D. Abràmoff, P. J. Magalhães, S. J. Ram, *Biophotonics international* **2004**, 11, 36.

4. APPENDIX

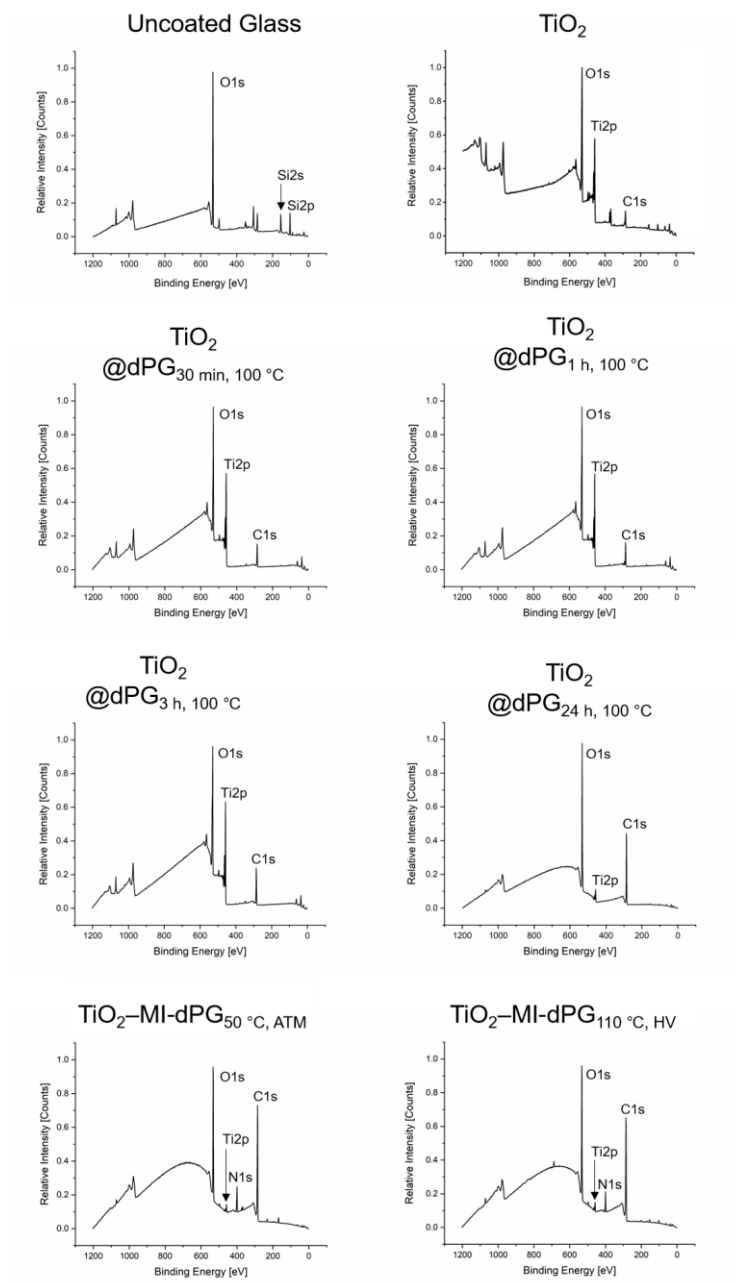


Figure S9. The XPS survey spectra of bare glass (which was used as the substrate material for the immobilization of TiO_2 and PDMS), TiO_2 , $\text{TiO}_2@\text{dPG}_{\Delta t}$, $100\text{ }^\circ\text{C}$, $\text{TiO}_2\text{--MI-dPG}_{50\text{ }^\circ\text{C, ATM}}$, and $\text{TiO}_2\text{--MI-dPG}_{110\text{ }^\circ\text{C, HV}}$.

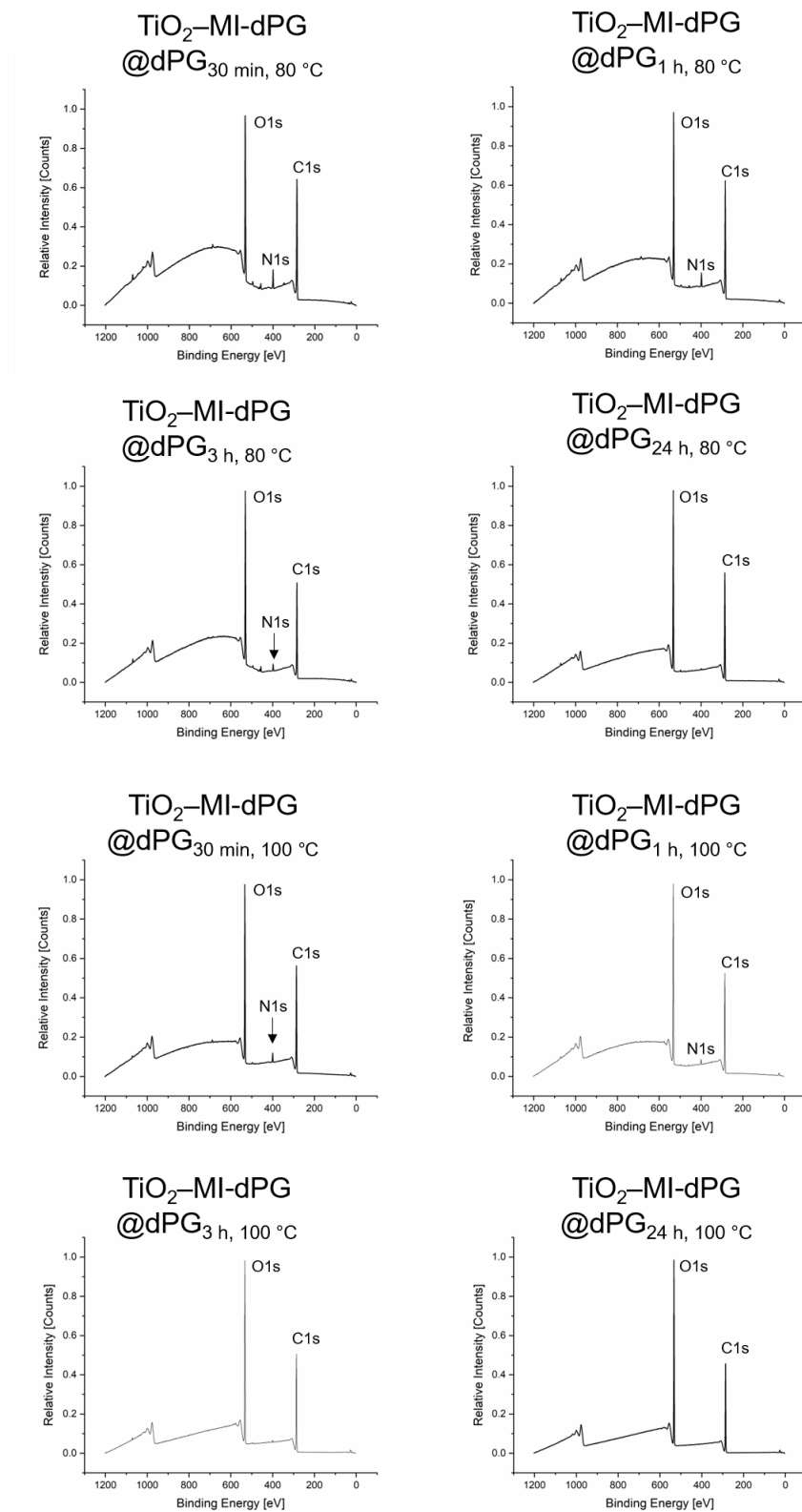


Figure S10. The XPS survey spectra of $\text{TiO}_2\text{-MI-dPG@ dPG}_{\Delta t, 80^\circ\text{C}/100^\circ\text{C}}$.

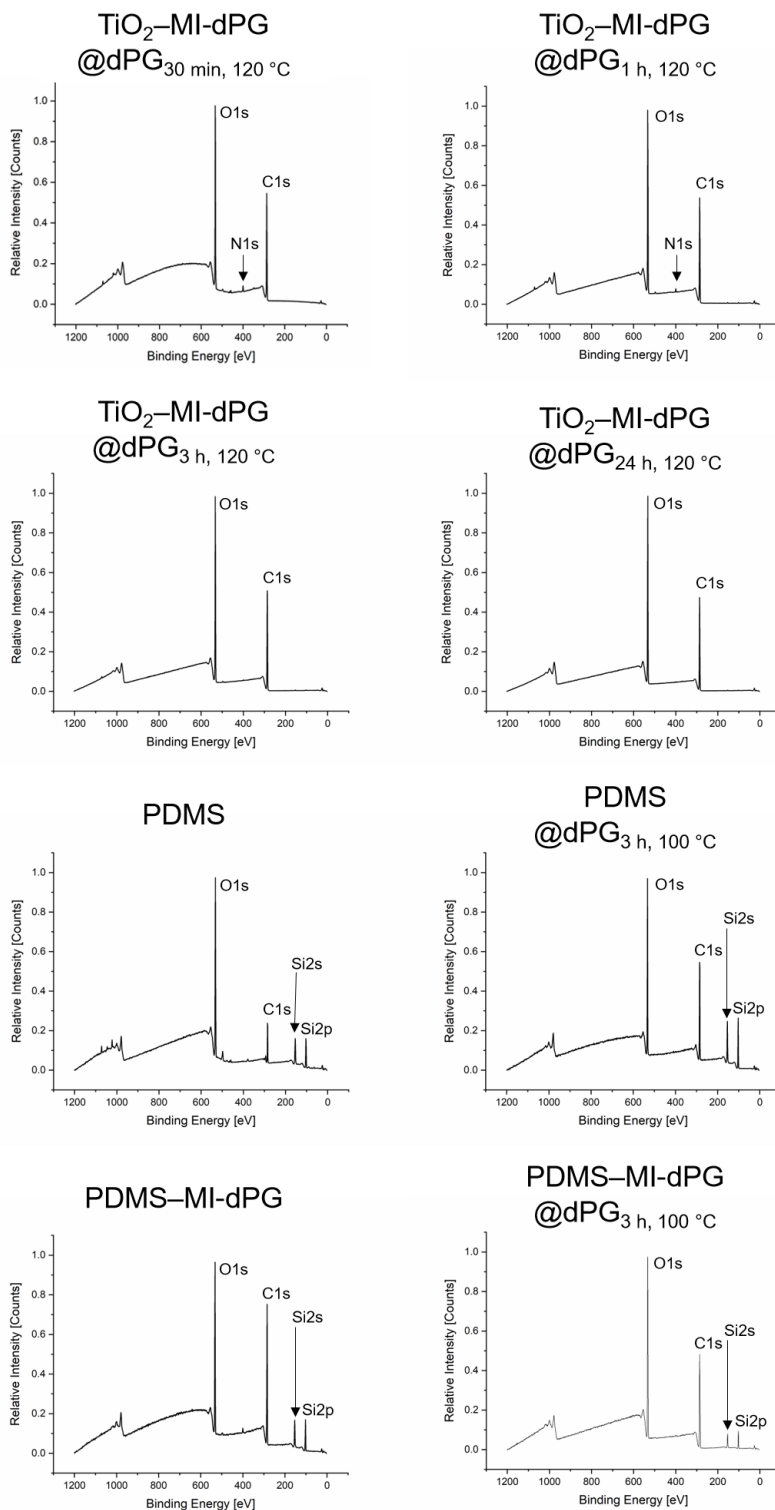


Figure S11. The XPS survey spectra of $\text{TiO}_2\text{-MI-dPG@dPG}_{\Delta t}$, $120\text{ }^\circ\text{C}$, PDMS, PDMS@dPG_{3 h}, $120\text{ }^\circ\text{C}$, PDMS-MI-dPG, and PDMS-MI-dPG@dPG_{3 h}, $120\text{ }^\circ\text{C}$.